2008 IEEE International Conference on
Robotics and Automation
Pasadena, CA, USA, May 19-23, 2008

On the Kinematics of Human Wrist during Pointing Tasks with Application to Motor Rehabilitation

Domenico Campolo, Dino Accoto, Fabrizio Taffoni and Eugenio Guglielmelli

***Abstract*— In this work, the kinematics of the human wrist during pointing tasks is assessed and discussed, especially in relation to the use of wrist robots.**

First, the existence of intrinsic kinematics constraints (or Donders' law, similarly to oculomotor system) for the human wrist during pointing tasks is verified. To this end, a novel approach based on a hand-held device is presented which allow assessing wrist movements without any mechanical loading.

Second, similar pointing tasks are assessed by means of a state-of-the-art wrist robot, typically used in robot-mediated therapy as well as assessment tool.

By comparing experimental results relative to the pointing task performed by healthy subjects with the hand-held device and with the robot, a loading effect on the performance due to the mechanisms of the robot is remarked. A functional requirement for the next generation of rehabilitation robots is thus provided.

***Index Terms*— Donders Law, Intrinsic Kinematic Constraints, Human Motor Control, Wrist Robots**

I. Introduction

Recent years have witnessed an increase of interest in robot-mediated motor therapy. Rehabilitators have focused increasing attention on the quantitative evaluation of residual motor abilities in the effort to obtain an objective evaluation of rehabilitation and pharmacological treatment effects, especially after the acute phase of recovery following traumatic brain injuries such as stroke. In the last two decades, various robots have been proposed which specifically target different areas of rehabilitation, ranging from upper to lower limbs, from proximal to distal joints. In 1991, a novel robot (MIT-MANUS, [6]) was proposed as a test bed to study the potential of using robots to assist in and quantify the neuro-rehabilitation of motor function. MIT-MANUS is a 2 DOF (Degrees Of Freedom) planar robot, specifically designed for the rehabilitation of shoulder and elbow. A typical session with the robot consists of a 'video-game' [6] which guides the patient through 2-dimensional planar motor tasks (e.g. vertical, horizontal and diagonal movements from/to the central position to/from a peripheral one) with the upper limb while the patient's hand grasps a handle attached to the robot end-effector. The robot might be programmed to exert force-fields, for example to help or to contrast the patient in specific situations.

More recently, an extension of the MIT-MANUS robot became available which also allows *wrist rehabilitation* [10]. Such a *wrist module* is a rotational 3 DOF robot, specifically designed to kinematically conform to the natural rotations of human wrist as well as to generate programmable torque-fields used during rehabilitation. Typical rehabilitation sessions for the wrist module also make use of 'video-games' as the one in Fig. 1: the patient, attached to a handle and with his/her torso, upper and lower arm fastened to an arm support, performs *pointing* tasks towards targets in the video-game (from/to the central target to/from the peripheral ones) with the only use of the 3 DOF wrist kinematics. In the case of the planar robot, a one-to-one correspondence exists between movements in the displayed video-game and the movements of the end-effector. In the case of the wrist module, a redundancy problem arises since more solutions are available to the motor system to solve the task since uncountably many elements of the 3-dimensional space of wrist configurations correspond to the same solution in terms of (2-dimensional) pointing task.

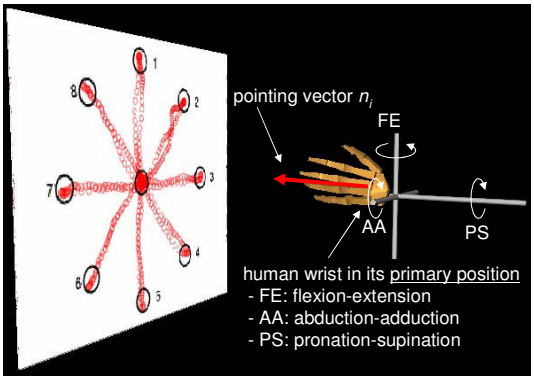

Fig. 1. Typical 'video-game' for guiding a subject through pointing tasks.

This problem closely resembles the one of *eye movements*, studied since the mid of the 19th century. In a good approximation, the eye can be considered as a center-fixed sphere rotated by the action of 6 (i.e. 3 agonist-antagonist couples) extra ocular muscles (EOMs). EOMs provide 3 DOF kinematics allowing full mobility in the space of rigid body rotations ($SO(3)$, see next section) with only limitations given in terms of range of motion.

Pointing tasks for the human wrist are kinematically similar to gazing tasks for the oculomotor system. When looking at some point in space, the gaze direction is fully determined but not the amount of ocular torsion about the line of sight. In other words, for a given line of sight, uncountably many eye configurations exist which correspond to the same gaze direction.

In 1847, Donders experimentally found that for a given *steady* gaze direction there is only one eye configuration

All the authors are with the Biomedical Robotics Laboratory of Campus Bio-Medico University, via Alvaro del Portillo, 21, 00128 Rome, Italy.
Corresponding author: d.campolo@unicampus.it

(*Donders' Law*) [9]. In other words, physiological eye positions are described by a 2-dimensional surface embedded into the 3-dimensional space of eye configurations: a solution to redundancy. Two decades later, Listing and Helmholtz went one step further, determining that such a 2-dimensional surface is actually a *plane*: the eye assumes only those positions that can be reached from primary position by a single rotation about an axis in *Listing's plane*, which lies orthogonal to the gaze direction in primary position (*Listing's Law*) [9].

In the last two decades, Donders' and Listing's laws have been found to well represent intrinsic strategies of the motor system in areas that range from eye movements (both for saccades and smooth pursuit) to head and limb movements, the reader is referred to [2] for a comprehensive collection of such works as well as to more recent papers such as [7] and references therein.

The goal of this paper is twofold: i) verifying the existence of a Donders' law, or intrinsic kinematic constraint, also for the human wrist during pointing tasks, in particular quantifying such a constraint in terms of 2-dimensional surfaces embedded in the 3-dimensional configuration space of the human wrist; ii) checking whether current state-of-the-art robots for motor therapy, when used as an assessment tool, comply with such an intrinsic constraint, providing recommendations for the next generation of rehabilitation robots.

Before proceeding, basic mathematical tools for describing the geometry of rotations will be briefly reviewed, the reader is also referred to [5], [3], [4].

II. Rotations, Gimbals and Wrist Kinematics

Rotations in the Euclidean space $\mathbb{R}^3$ can be described by the *group* of 3×3 orthonormal matrices:

$$SO(3) = \{R \in \mathbb{R}^{3\times 3} : R^T R = I, \det R = +1\}$$

where I is 3×3 identity matrix. Any orientation $R \in SO(3)$ is equivalent to a rotation about a fixed axis $\mathbf{v} \in \mathbb{R}^3$ through an angle $\theta \in [0, 2\pi)$ [8, Euler's Theorem].

A rotation matrix R can be seen as a mapping $R : \mathbb{R}^3 \rightarrow \mathbb{R}^3$ and represented in $\mathbb{R}^3$ (i.e. the same space it acts upon) via a *rotation vector* $\mathbf{r} = [r_x, r_y, r_z]^T \in \mathbb{R}^3$ which defines the axis (parallel to $\mathbf{r}$ itself) and the amount of rotation ($\|\mathbf{r}\| = \tan(\theta/2)$). As shown in [3], for a generic rotation R, the corresponding rotation vector is:

$$\mathbf{r} = \frac{1}{1 + R_{1,1} + R_{2,2} + R_{3,3}} \begin{bmatrix} R_{3,2} - R_{2,3} \\ R_{1,3} - R_{3,1} \\ R_{2,1} - R_{1,2} \end{bmatrix} \quad (1)$$

where $R_{i,j}$ represents the (i, j) element of the matrix R.

Rotations about principal axes (x-, y- and z-axis) can be written as:

$$R_x(\theta) = \begin{bmatrix} 1 & 0 & 0 \\ 0 & \cos\theta & -\sin\theta \\ 0 & \sin\theta & \cos\theta \end{bmatrix} \quad (2)$$

$$R_y(\theta) = \begin{bmatrix} \cos\theta & 0 & \sin\theta \\ 0 & 1 & 0 \\ -\sin\theta & 0 & \cos\theta \end{bmatrix} \quad (3)$$

$$R_z(\theta) = \begin{bmatrix} \cos\theta & -\sin\theta & 0 \\ \sin\theta & \cos\theta & 0 \\ 0 & 0 & 1 \end{bmatrix} \quad (4)$$

For solving a pointing task, only 2 DOF would suffice.

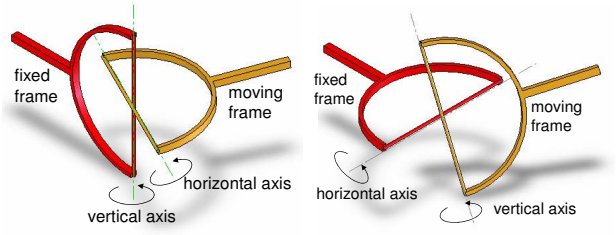

Fick-gimbal Helmholtz-gimbal

Fig. 2. Gimbals

Examples of mechanical systems with 2 DOF are the Fick's and Helmholtz's gimbals in Fig. 2, where the order of rotation (of an angle θ_v about the vertical axis and θ_h about the horizontal axis) is mechanically imposed by the structure of the system:

$$R_{Fick} = R_z(\theta_v)R_y(\theta_h) \quad (5)$$

$$R_{Helm} = R_y(\theta_h)R_z(\theta_v) \quad (6)$$

One of the main characteristics of $SO(3)$ is the *non-commutativity* property of the group since. in general, $R_{Fick} \neq R_{Helm}$, i.e. in a sequence of rotations, the order matters. In general, the couple of angles (θ_v, θ_h) that leads to a given pointing direction, would be different according to whether a Fick-gimbal or a Helmholtz-gimbal is used.

Via straightforward calculations, it can be verified that for Fick and Helmholtz gimbals the following hold:

$$\begin{array}{ll} r_x = -r_y\, r_z & (Fick) \\ r_x = +r_y\, r_z & (Helmholtz) \end{array} \quad (7)$$

where r_x, r_y and r_z represent the components of $\mathbf{r}$, the rotation vector derived, respectively, from R_{Fick} and R_{Helm} according to Eq. (1).

Equations (7) represent, respectively for the Fick and the Helmholtz gimbals, constraints for the achievable orientations. In particular, in the 3-dimensional $SO(3)$ space, only those orientations can be achieved whose rotation vectors lie on the surfaces defined by the quadratic forms in Eq. (7). Of course, this was expected since the mechanical structures of the Fick and Helmholtz gimbals only allow 2 DOF and this translates into a 2-dimensional manifold embedded in $SO(3)$.

On the other hand, the existence of a 2-dimensional manifold (i.e. Donders' and Listing's laws) for a 3 DOF systems such as the human eye is remarkable, since it denotes a *simplifying* strategy of the motor system. In the last decade, a number of works have shown the existence of Donders' and

Listing's laws in the case of head and limbs movements, in specific situations. Validation of such an hypothesis for the kinematics of human wrist during pointing tasks is the focus of next section.

III. Donders' Law for the Human Wrist

In this section, the proposed methodology and experimental setup devised to test the hypothesis that intrinsic kinematic constraints, such as Donders' law, can account for the geometric features of 3-dimensional wrist movements during pointing tasks are presented.

A. Materials and Methods

Subjects: Three healthy subjects, aged between 28 and 33 years old, were asked to complete a series of pointing tasks.

Apparatus: Each subject was strapped to a chair and to an arm-support by appropriate belts to minimize torso, shoulder and elbow movements, so that only wrist rotations were left unconstrained. The orientation $R \in SO(3)$ of the wrist was measured by means of a commercial Inertial Magnetic Unit (IMU, MTx-28A33G25 device from XSens Inc.) mounted on top of a hollow cylindrical handle (height: 150mm, outer diameter: 50mm, inner diameter: 35mm) which each subject was asked to grasp firmly during the experiment. In what follows, such an apparatus is referred to as *hand-held* device.

The IMU, connected to a PC, was configured to continuously acquire the sequence of orientation matrices R_i at a rate of 100 samples/sec. Performance of the selected commercial IMU in terms of static orientation accuracy ($< 1^o$) and sensing bandwidth (40 Hz) is more than adequate considering the kinematic requirements of the motor task

Each subject, before starting each pointing task, was asked to hold still in a posture of the wrist which would allow, according to the subject's perception, equal positive and negative excursions in terms of flexion-extension, adduction-abduction, and pronation-supination. This 'zero' position defined the *primary position*, which was found to have inter-subjective differences as well as minor differences from task to task for the same subject.

With the wrist in the primary position, a fixed reference frame $\{x_0, y_0, z_0\}$ was defined as:

- z_0*-axis*: along the vertical direction (upwards);
- x_0*-axis*: horizontal, aligned with the forearm (forward);
- y_0*-axis*: horizontal and perpendicular to the forearm (leftward).

A second reference frame $\{x, y, z\}$ attached to the wrist (moving frame) was defined so to coincide with the fixed reference frame when the wrist is in the primary position.

In order to reduce computational complexity, the primary position was also selected as the 'home' position for the IMU, meaning that the coordinates of the x, y, and z axes with respect to the fixed frame $\{x_0, y_0, z_0\}$ could be determined as, respectively, the first, the second and the third column of the matrix R_i. To this aim, a software *reset procedure* for the IMU device must be performed while the wrist is held still in the primary position.

For a generic orientation R_i, the *pointing vector*, (always parallel with the moving x-axis after the reset procedure) can then be determined as the first column of R_i:

$$\mathbf{n}_i = R_i \, [1 \; 0 \; 0]^T \tag{8}$$

A computer screen was used to display the 'videogame' according to the protocol below where (see Fig. 1) the position of a round cursor is determined, in real-time, directly by the orientation of the subject's wrist. In particular, the screen was physically located on the vertical plane in front of the subject (the y_0-z_0 plane) and the position of the cursor was determined by the projection of the pointing vector $\mathbf{n}_i$ onto the y_0-z_0 plane. The position of the cursor is given by the second and the third components of the vector $\mathbf{n}_i$. A rotation of 30^o (≈ 0.5 rad) of the wrist is required to move the cursor from the central position to any of the peripheral positions in Fig. 1.

Protocol: The session starts with the subject in the primary position and, therefore, with the cursor projected onto the central position. The subject is then instructed to move the round cursor on the screen towards the peripheral position '1' in Fig. 1 and then back to the central position. The same task is then repeated for positions '2', '3' ... '8'. This completes a single trial.

After an initial trial used for the subject to get acquainted with the experimental setup, each subject is asked to repeat the trial 4 times.

B. Experimental Results for the Hand-Held Device

The sequences of rotation matrices R_i acquired during each trial performed by the 3 subjects were analyzed as follows.

Given the sequence R_i relative to each trial, the sequence of rotation vectors $\mathbf{r}_i$ and the sequence of pointing vectors $\mathbf{n}_i$ were derived via eq. (1) and eq. (8), respectively. As an example, both sequences of a single trial are plotted in Fig. 3. It is worth here recalling the *geometrical* interpretation of

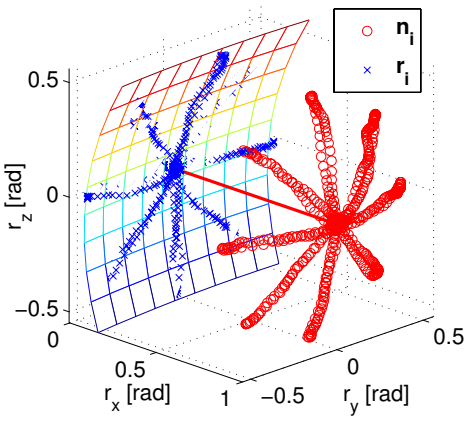

Fig. 3. Rotation vectors (crosses) are represented (in radiants) in the 3-dimensional space of the motor task together with the pointing vectors (circles). A 2-dimensional quadratic surface (Donders' surface) fits the rotation vectors with a 0.029 rad (1.67^o) deviation (thickness).

$\mathbf{r}_i$: at any time t_i, the orientation R_i of the wrist can be achieved from the primary position by a *single rotation* about the vector $\mathbf{r}_i$ of an angle $\theta_i = 2\arctan(\|\mathbf{r}_i\|)$. Such an interpretation allows representing rotations in the same 3-dimensional space of the motor task. In Fig. 3, both the wrist pointing directions $\mathbf{n}_i$ (circles) and the rotation vectors[1] $\mathbf{r}_i$ (crosses) are represented. While the wrist pointing directions necessarily lie in a 2-dimensional space[2], the three components r_{xi}, r_{yi} and r_{zi} of a rotation vector $\mathbf{r}_i$, in general, define points of a 3-dimensional space. Remarkably, it can be observed that the rotation vectors tend to lie on a 2-dimensional surface (Donders' law) which can be well approximated by a plane (Listing's law) near the primary position. This verifies the hypothesis of existence of Donders' law for the human wrist, during pointing tasks.

Numerically, the sequence $\mathbf{r}_i = [r_{xi}\ r_{yi}\ r_{zi}]^T$ was fitted as in [9] with a generic quadratic surface:

$$r_{xi} = C_1 + C_2 r_{yi} + C_3 r_{zi} + C_4 r_{yi}^2 + 2C_5 r_{yi} r_{zi} + C_6 r_{zi}^2 \quad (9)$$

where the coefficients $C_1 \dots C_6$ were determined via nonlinear least-squares fitting methods[3]. The first three coefficients (C_1, C_2 and C_3) define a plane (Listing's plane), while the last three coefficients (C_4, C_5 and C_6) are related to the *curvature* of the fitted surface, see [1]. In particular, the coefficient C_5 denotes the amount of *twisting* of a quadratic surface.

Deviation from the best fitting surface, i.e. the *thickness* of a Donders' surface, is defined as the standard deviation of the sequence $\mathbf{r}_i$ from eq. (9).

In Fig. 5, results relative to the three subjects are presented in terms of Donders' surfaces as well as in terms of histograms of the $C_1 \dots C_6$ coefficients for each trial. In particular, thicknesses in the order of $1 - 3^o$ for angular excursions of 30^o are found, in line with deviations found in the oculomotor system [9] or for the upper limbs [7].

It is worth noting how simply the kinematic analysis allows to clearly identify a personal motor 'style' for each subject, i.e. a different motor strategy throughout the execution of the 4 motor trials in terms of curvature (C_4 and C_6) and twisting (C_5) of the Donders' surfaces.

IV. Donders' Law for the Human Wrist when Connected to a Wrist Robot

In this section, Donders' law for the human wrist during pointing tasks is analyzed when the wrist is connected to wrist robot, in particular the wrist extension module of the MIT-MANUS robot. Such a robot, generally used for therapy, is equipped with motors that can generate programmable torque-fields. Robots interacting with humans are in general very different from industrial robots, especially as long as mechanical loading and back-drivability[4] issues are concerned. When used for *assessment*, the robots should not influence the human performance.

In this work, the motors of the robot are excluded (turned-off) in order to study the effects of mechanical loading of the robot mechanisms on the kinematics of the human wrist.

A. Materials and Methods

Subjects: three healthy subjects, were asked to complete a series of pointing tasks.

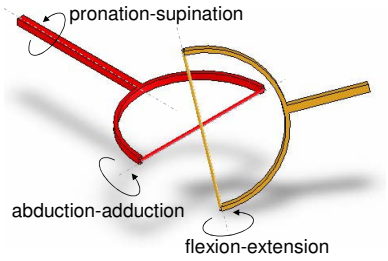

Fig. 4. Mechanism of the wrist robot as derived from [10]

Apparatus: each subject, one at a time, was strapped to a chair and to an arm-support by appropriate belts to minimize torso, shoulder and elbow movements, only wrist rotations were left unconstrained. The subject was then attached to the wrist module of a MIT-MANUS robot [10]. The wrist module consists of a mechanism which is able to conform to wrist rotations once the forearm of the subject is strapped onto the module and the subject grasps a handle, also part of the module. The sequence of mechanical joints that allow the mechanism to conform to the 3 DOF wrist rotations, as derived from [10], is represented in Fig. 4. In particular the following angles can be sensed (and actuated by the robot): $i)$ θ_{PS} (Pronation-Supination); $ii)$ θ_{AA} (Abduction-Adduction); $iii)$ θ_{FE} (Flexion-Extension). Knowledge of the sequence of the mechanical joints allows to determine the wrist orientation R_w from the angles as sensed by the wrist module:

$$R_w = R_x(\theta_{PS}) R_y(\theta_{AA}) R_z(\theta_{FE}) \quad (10)$$

where x, y and z refer to the principal axes of a reference frame initially (i.e. the primary or "zero" position) aligned with the forearm (x direction) and with the mechanical handle (z direction). For a given wrist orientation R_w, the *wrist pointing direction* $\mathbf{n}_w$ is given as in (8).

Protocol: once seated, each subject faces a computer screen where a 'video-game' as in Fig. 1 is displayed. The subject is then instructed about the task: starting from the central position, the cursor on the screen shall be moved towards the peripheral positions and then back to the central position, from position '1' to position '8'. The position of the cursor on the screen is determined in *real-time* from the

[1] In fact, vectors of length θ_i instead of $\|\mathbf{r}_i\|$ are represented so that the amount of rotation (in radiants) can be visually derived.

[2] Pointing vectors $\mathbf{n}_i$ are unit-length vectors and therefore their end-tips lie on a sphere as clear in Fig. 3.

[3] The function `nlinfit` in the MATLAB environment from MathWorks Inc. was used

[4] Back-drivability is the ability to move the end-effector in the workspace without opposition. A back.driveable mechanism is characterized by high kinematic efficiency (low friction losses) as well as low apparent inertia when back-driven. Back drivability is therefore typically hindered by friction in the motors and transmissions and by high ratio reduction gears and mechanisms.

wrist pointing direction $\mathbf{n}$. Although the MIT-MANUS wrist module allows actuation of the 3 DOF, this functionality was disabled by turning the motors off. Only at the system start, an off-setting procedure (linking the primary position of the wrist module with the central position in the video-game) requires the motors to be 'on'. In a single session, each trial is repeated 5 times but only the last 4 trials are considered for each subject since the first task seemed to be always influenced by the turning 'on' and 'off' of the motor relative to the pronation-supination angle (with no effect on the zero position of the video game but with off-setting effects on the natural, initial posture of the subjects).

B. Experimental Results for the Wrist Robot

In this section, the data from 3 subjects are analyzed and compared. During the execution of each task, data were acquired at a rate of 200 Samples/sec, in particular the three sequences of sampled angles θ_{PSi}, θ_{AAi}, and θ_{FEi} (where i refers to i-th sample at time t_i). Using eq. (10), the sequence of wrist orientation R_{wi} at time t_i was derived. The sequence of wrist pointing directions $\mathbf{n}_i$ was evaluated via eq. (8) and finally the sequence of rotation vectors $\mathbf{r}_i$ was obtained via eq. (1). The sequence $\mathbf{r}_i = [r_{xi}\ r_{yi}\ r_{zi}]^T$ was numerically fitted to a generic quadratic surface with coefficients $C_1 \dots C_6$ as in (9).

Donders' surfaces for the 3 subjects are shown in Fig. 6 where, for each subject, surfaces relative to the 4 trials are superimposed. The best fitting surfaces do not change significantly from trial to trial for the same subject. Slight differences exist among subjects and can be better appreciated in the bar-plots of the coefficients in Fig. 6.

V. Discussion of Results

By comparing results relative to the hand-held devices, in Fig. 5, with those relative to the wrist robot, in Fig. 6, it is evident that the robot mechanism strongly influences the subjects, losing thus a great deal of information about the personal 'style' of each subject.

Referring to Fig. 6, the influence of the mechanism is particularly evident in the Helmholtz-like behavior of the surfaces, i.e.

i) inter-subjectively invariant and positive sign of the C_5 coefficient;
ii) relatively small C_4 and C_6 coefficients.

It is worth recalling that the Fick and Helmholtz gimbals are 2-dimensional mechanisms and therefore their rotation vectors necessarily lie on 2-dimensional surfaces defined in eq. (7), a particular case of eq. (9) where all the coefficients are zero except for $C_5 = \pm 1/2$. In particular, for the Helmholtz gimbal $C_5 = 1/2$ holds. A possible explanation for this is that the pronation-supination axis of the robot, see Fig. 4, provides excessive mechanical loading (especially inertial) to the subject, limiting thus the natural torsion of the wrist. When the pronation-supination axis is blocked, the 3dof mechanism in Fig. 4 is actually equivalent to the Helmholtz gimbal in Fig. 2 (right).

VI. Conclusions

In this work the kinematics of the human wrist during pointing tasks is discussed with a twofold goal: i) verifying the existence of a Donders' law for the human wrist during pointing tasks (or whenever redundancy issues arise), similarly to what has been verified for other motor systems such as eyes, head and arms; ii) verifying whether state-of-the-art robots for wrist rehabilitation comply with such a law, defining thus a functional requirement for the new generation of rehabilitation robots.

The kinematics of the human wrist during pointing tasks was first assessed by means of a hand-held device that would not influence the performance of the subject. This allowed characterizing the performance of each subject by a specific Donders' surface, emphasizing thus a personal 'style'.

Second, similar tasks were repeated by means of a wrist robot (wrist extension of the MIT-MANUS). A similar analysis of the data was carried out and the results were compared with previous ones. Such a comparison denoted the large influence of the robot mechanisms on the performance of the subject, leading to inter-subjectively invariant behaviors, i.e. flattening out any personal 'style' in the performance of the task.

The ability not to modify the personal style (in the sense defined in this paper) in the performance of motor tasks is a functional requirement for the new generation of rehabilitation robots. In particular, as future work, the response of a subject to different mechanical loading conditions (a combination of inertia, friction and also stiffness) in terms of variations of Donders' surfaces will be studied. Such a knowledge could help defining subject-specific feedback laws in robot-mediated therapy which do not alter each subject's motor style.

References

[1] M. P. Do Carmo, *"Differential Geometry of Curves and Surfaces"*, Prentice Hall, June 1976.

[2] M. Fetter, T. Haslwanter, H. Misslich, D. Tweed (Eds), *"Three-dimensional Kinematics of the Eye, Head and Limb Movements"*, Amsterdam, The Netherlands, Harwood Academic Publisher, 1997.

[3] T. Haslwanter, *"Mathematics of Three-dimensional Eye Rotations"*, Vision Res. Vol. 35, No. 12, pp. 1727-1739, 1995.

[4] A. A. Handzel and T. Flash, *"The geometry of eye rotations and listing's law"*. In D. Touretzky, M. Mozer, and M. Hasselmo, (Eds), *"Advances in Neural Information Processing Systems 8"*, Cambridge, MA., MIT Press, pp. 117-123, 1996.

[5] K. Hepp, *"On Listing's Law"*, Commun. Math. Phys., Vol. 132, pp. 285-292, 1990

[6] H. I. Krebs, N. Hogan, M. L. Aisen, and B. T. Volpe, *"Robot-Aided Neurorehabilitation"*, IEEE Trans. Rehabil. Eng., Vol. 6, No. 1, pp. 75-87, Mar. 1998.

[7] D. G. Liebermann, A. Biess, J. Friedman C. C. A. M. Gielen, T. Flash, *"Intrinsic joint kinematic planning. I: Reassessing the Listing's law constraint in the control of three-dimensional arm movements"*, Exp. Brain. Res., Vol. 171, pp. 139-154, 2006.

[8] R. M. Murray, Z. Li, and S. S. Sastry, "*A Mathematical Introduction to Robotic Manipulation*", CRC, Boca Raton, FL, 1994.

[9] D. Tweed and T. Vilis, *"Geometric Relations of Eye Position and Velocity Vectors during Saccades"*, vision Res., Vol. 30, No. 1. pp. 111-127, 1990.

[10] D. J. Williams, H. I. Krebs, N. Hogan, *"A Robot for Wrist Rehabilitation"*, in Proc. of 23rd EMBS Intl Conf, pp. 1336-1339, Istanbul, Turkey, Oct. 25-28, 2001.

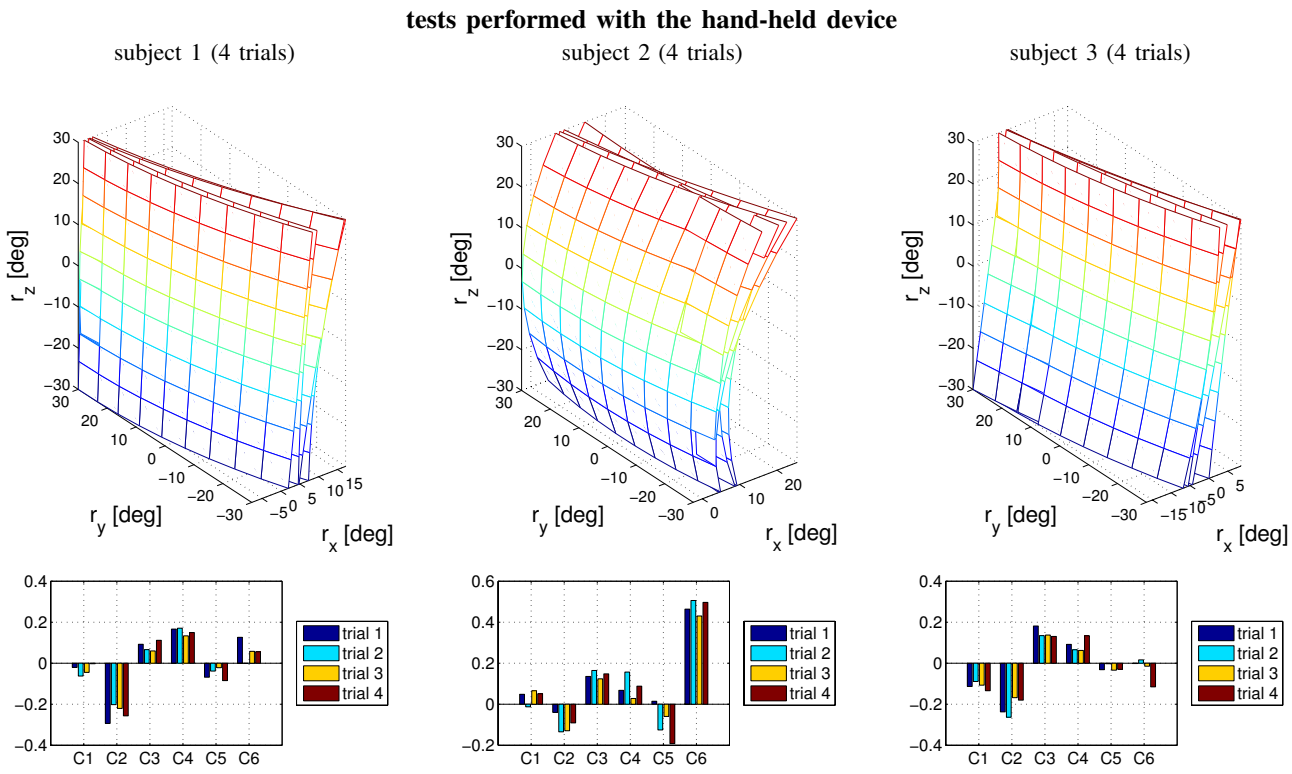

Fig. 5. Experimental data relative to the tests performed with the hand-held device. Each column represents a subject. Top row: superimposed Donders' surfaces fitting the rotation vectors (in degrees) for the 4 trials of a single subject. Bottom row: histogram of the $C_1 \ldots C_6$ coefficients fitting each of the 4 trials.

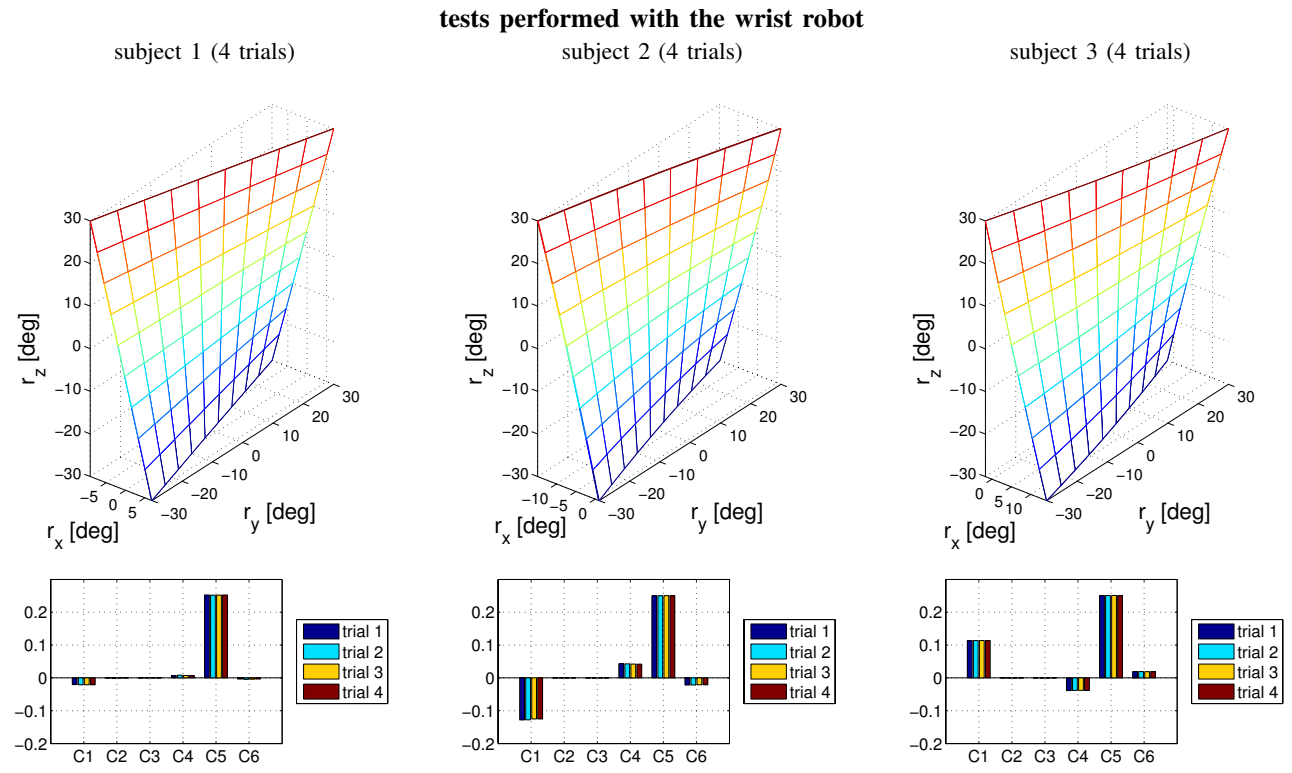

Fig. 6. Experimental data relative to the tests performed with the wrist robot. Each column represents a subject. Top row: superimposed Donders' surfaces fitting the rotation vectors (in degrees) for the 4 trials of a single subject. Bottom row: histogram of the $C_1 \ldots C_6$ coefficients fitting each of the 4 trials.